J3.4

LAGRANGIAN MODELING OF DISPERSION IN THE STABLE BOUNDARY LAYER

Jeffrey C. Weil[1]*, Edward G. Patton[2], and Peter P. Sullivan[2]

[1]Cooperative Institute for Research in Environmental Sciences, University of Colorado, Boulder, CO
[2]National Center for Atmospheric Research, Boulder, CO

1. INTRODUCTION

Current knowledge of dispersion in the stable boundary layer (SBL) is far from complete and indeed much less so than for its convective counterpart. For the SBL, dispersion from surface releases is the most well-understood and documented case thanks to theoretical work (e.g., Horst, 1979; van Ulden, 1978) and field observations, most notably the Prairie Grass experiment (Barad, 1958). However, for sources above the surface, the situation is less clear due to insufficient observations and information on the turbulence structure. Theories exist for the vertical dispersion of elevated plumes—standard statistical theory (Taylor, 1921; Venkatram et al., 1984), an alternative statistical model for stable environments (Pearson et al., 1983), and eddy-diffusion (K) theory (Nieuwstadt, 1984a). The main challenge is knowing the conditions under which they apply and having the required turbulence information.

Large-eddy simulation (LES) is a promising tool for investigating turbulence and dispersion in the SBL. A number of LESs have been conducted (e.g., Beare et al., 2005; Brown et al., 1994; Kosovic and Curry, 2000), but they have been restricted to a weakly stable boundary layer (WSBL), which is characterized by moderate-to-strong winds, weak surface cooling, and a continuously turbulent layer. The key restriction is to continuous (i.e., non-intermittent) turbulence. The above LESs and the one used here (Moeng and Sullivan, 1994; Sullivan et al., 1994) have reproduced several SBL features including a low-level jet, a triple-layer potential temperature structure, and realistic turbulence profiles.

We investigate dispersion in the SBL using a Lagrangian particle model driven by velocity fields from LES. In this approach, one follows passive particles in a turbulent flow given the random velocity field and finds the ensemble-mean concentration by simulating thousands of particle trajectories; the mean concentration is proportional to the probability density function (PDF) of particle position. The approach has been applied suc-

cessfully to the convective boundary layer (CBL) (e.g., Lamb, 1978; Weil et al., 2004) and informative SBL results were presented earlier by Kemp and Thomson (1996). Here, we report on dispersion for a range of source heights in the SBL.

2. NUMERICAL MODELS

2.1 Large-eddy simulations

The velocity fields used here were obtained using the Moeng and Sullivan (1994) and Sullivan et al. (1994) models but modified to address an SBL. They were generated originally as part of the GABLS (Global Energy and Water Cycle Experiment Atmospheric Boundary Layer Study) initiative (Beare et al., 2005). The simulations were conducted with a 400 m $\times$ 400 m $\times$ 400 m domain, $200 \times 200 \times 192$ grid points, with a grid resolution of ~ 2 m; the geostrophic wind speed was 8 ms^{-1}, the surface cooling rate was 0.25 °Khr^{-1}, and the surface friction velocity u_* was ~ 0.28 ms^{-1}. The stability index z_i/L was 1.6, where z_i ($= 200$ m) and L are the SBL height and M-O length, respectively; the potential temperature gradient in the bulk of the layer was $\partial\Theta/\partial z \simeq 0.006$ °Cm^{-1}, but it was greater near the surface and SBL top, thus producing a triple-layer structure of the mean potential temperature Θ.

2.2 Lagrangian particle model

In Lagrangian dispersion models, passive "particles" released in a turbulent flow are assumed to behave as fluid elements and to travel with the local fluid velocity with molecular diffusion ignored. The mean concentration C is found from

$$C(\mathbf{x},t) = Q \int_{-\infty}^{t} p_1(\mathbf{x},t;\mathbf{x}_s,t')dt' \qquad (1)$$

where Q is the source strength, $\mathbf{x}$ is the position vector (indicated by a boldface symbol), and $p_1(\mathbf{x},t;\mathbf{x}_s,t')$ is the position PDF of material released at the source position $\mathbf{x}_s$ at time t' being found at $\mathbf{x}$ at time t. p_1 is computed from the numerically-calculated particle trajectories.

*corresponding author address: Jeffrey C. Weil, National Center for Atmospheric Research, P. O. Box 3000, Boulder, CO 80307-3000; email: weil@ucar.edu
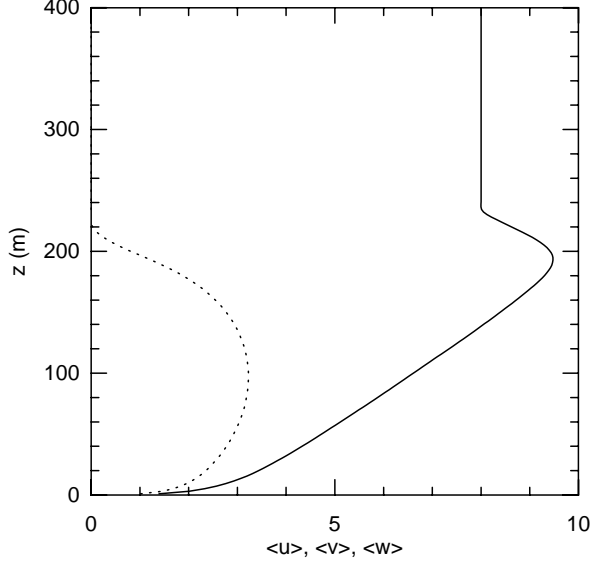
Figure 1: Mean wind profiles in the stable boundary layer; solid curve is $\langle u \rangle$ and dotted line is $\langle v \rangle$.

Figure 2: Mean variance profiles in the stable boundary layer; solid, dotted, and dashed-dot curves are for the u, v, and w components, respectively.

The particle position $\mathbf{x}_p$ is found by integrating $d\mathbf{x}_p = \mathbf{u}_L dt$, where $\mathbf{u}_L$ is the Lagrangian velocity of the particle. The $\mathbf{u}_L$ is decomposed as

$$\mathbf{u}_L(\mathbf{x}_p, t) = \mathbf{u}_r(\mathbf{x}_p, t) + \mathbf{u}_s(\mathbf{x}_p, t) \qquad (2)$$

where $\mathbf{u}_r$ is the LES resolved velocity at $\mathbf{x}_p(t)$ and t, and $\mathbf{u}_s$ is a random subfilter-scale (SFS) or subgrid-scale velocity. This method was first adopted by Lamb (1978). Our approach is similar to his except for a more detailed stochastic SFS or $\mathbf{u}_s$ model (Weil et al., 2004) (as used in the CBL).

The mean crosswind-integrated concentration (CWIC) is given by $C^y = \int_{-\infty}^{\infty} C(x, y, z) dy$, where x, y, and z are the distance downstream of the source, lateral distance from the mean plume centerline, and height above ground. The mean CWIC fields were obtained by superposing the position PDFs (p_1) from 289 equally-spaced sources at height z_s in a horizontal plane. At each source, 50 particles were released, each with a random initial SFS velocity. The releases were made at 5 equally spaced times over a 2.5-min period, resulting in a total of 72,250 particles released; sensitivity studies were made for a 5-min release as discussed below.

3. RESULTS

3.1 Mean wind, turbulence, and eddy diffusivity

The key variable driving the particles in the Lagrangian trajectory calculations is the resolved velocity field. Figure 1 shows the mean resolved velocity profiles,

where $\langle u \rangle$ and $\langle v \rangle$ are the east-west and north-south components, respectively; the angle brackets denote an ensemble mean, which is obtained by averaging over time as well as the $x - y$ plane. The $\langle u \rangle$ shows substantial shear over the entire boundary layer and culminates in the jet just below z_i. The variation of $\langle v \rangle$ with height leads to an Ekman spiral, which has an important effect on the mean lateral particle transport and dispersion as discussed below. The above mean profiles are similar to those produced by other LESs (Brown et al., 1994; Kosovic and Curry, 2000).

Figure 2 presents the resolved velocity variances $\langle u^2 \rangle$, $\langle v^2 \rangle$, $\langle w^2 \rangle$, which all show a monotonic decrease with height as expected. The maximum total velocity variances, e.g., $\langle w_{mt}^2 \rangle$, near the surface are consistent with the measurements of Nieuwstadt (1984b) for the w component and with other measurements and LESs for the u and v components. The $\langle w_{mt}^2 \rangle = \langle w^2 \rangle + (2/3)\langle e_s \rangle$, where $\langle e_s \rangle$ is the mean SFS TKE at the height of the w variance maximum. We find that the maximum values are $5u_*^2$, $4u_*^2$, and $2u_*^2$ for the u, v, and w components, respectively.

A simple parameterization for the vertical eddy diffusivity of a scalar, K_z, was assessed to provide guidance on the relevant Lagrangian integral time scale, T_L, for analyzing the vertical dispersion results in Section 3.2. Based on the work of Brost and Wyngaard (1978) and Wyngaard (1988), the turbulence length (ℓ) and time (T_L) scales in the upper part of the SBL are expected to be small in the sense that $\ell/z_i \ll 1$ and $T_L u_*/z_i \ll 1$. In this case, the diffusivity should be given by the long-time
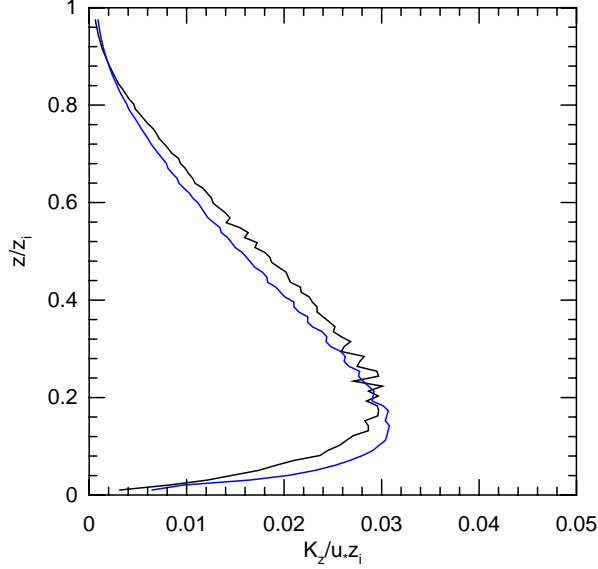
Figure 3: Eddy diffusivity profiles as a function of dimensionless height with K_θ (black curve) and K_z (blue curve) computed from LES variables; for K_z, $a = 0.2$.

limit of Taylor's theory (Taylor, 1921), $K_z = \sigma_w^2 T_L = \sigma_w \ell$, where $\ell = \sigma_w T_L$. The limiting ℓ in the upper part of the SBL is the buoyancy length $\ell_b \sim \sigma_w / N$, and the $T_L \sim N^{-1}$ (Wyngaard, 1988); here, $N = [(g/T_o)(\partial\Theta/\partial z)]^{1/2}$ is the Brunt-Vaissala frequency, where g is the gravitational acceleration, and T_o is the mean absolute temperature. Thus, the expected form of K_z is $K_z = a\sigma_w^2 N^{-1}$, where a is a constant.

The above K_z can be tested for its relevance here using the diffusivity for heat, K_θ, computed from the LES; the K_θ was obtained from $K_\theta = -\langle w\theta \rangle / (\partial\Theta/\partial z)$ using the computed heat flux $\langle w\theta \rangle$ and $\partial\Theta/\partial z$. Figure 3 compares the parameterized K_z (blue curve) with the K_θ, where σ_w^2 and N also are found from the LES. A least-squares-fit of the K_z to K_θ resulted in $a = 0.2$, which is included in the K_z (Fig. 3). As can be seen, the K_z provides a good overall shape to the K_θ profile, thus reinforcing the choice of ℓ_b and N^{-1} as the relevant length and time scales.

3.2 Dispersion from surface and elevated sources

In this section, we analyze fields of the CWIC, the vertically-integrated concentration, and the plume dispersion or displacement statistics. The CWIC is nondimensionalized by $Q/(Uz_i)$, which is the (vertically) uniformly mixed C^y value far downstream, and U is the magnitude of the vertically-averaged wind vector over the boundary layer with $U = 7$ ms^{-1}. (x and y are re-oriented for the transport and dispersion calculations to have x in the direction of the vector-averaged wind over the SBL, and y is normal to x in the horizontal plane.)

Two time or distance scalings are used in the following. The first is analogous to CBL scaling and is the dimensionless distance (show a range of results for a range of heights)

$$X = \frac{u_* x}{U z_i}, \tag{3}$$

where the friction velocity replaces the convective velocity scale for CBL analysis; X is the ratio of a mean travel time x/U to the maximum eddy turnover time (z_i/u_*) that could exist in the SBL. The second dimensionless time or distance is $tN^{-1} = x/(UN)$.

Figure 4 shows the dimensionless CWIC as a function of z/z_i and X for a surface source in the SBL. For reference, the distance scale Uz_i/u_* used in scaling the distance x is $\simeq 5100$ m, and the panels shown in Fig. 4 are for $x = 916, 1832, 2448, 3665$, and 4581 m. The vertical evolution of the CWIC profiles is quite slow by comparison to that in the CBL due to the much smaller turbulence scales in the SBL—σ_w for velocity and ℓ_b for length. For example, at $X = 0.72$, the profile is contained in the lower half of the boundary layer with a maximum CWIC of about $6Q/(Uz_i)$ (at the surface), whereas for the CBL at the same X, the plume has dispersed to the CBL top and the maximum CWIC is only about $1.4Q/(Uz_i)$

For comparison, Fig. 5 shows the evolution of the CWIC profiles with downwind distance or X for an elevated source at $z_s/z_i = 0.24$. The initially compact plume $(X = 0.18)$ has a maximum CWIC near the source height that is only about a third of the maximum for the surface source at the same X. This is attributed to the much higher wind speed aloft than at the surface; the higher speed leads to a greater dilution of the plume through $C^y \propto Q/(U_s \sigma_z)$, where U_s is the mean wind speed at z_s, and σ_z is the local root-mean-square (rms) spread about the plume height. In addition, the CWIC profiles exhibit a more rapid downward than upward dispersion about the plume centerline; this is caused by the stronger turbulence below the source than above it.

One consequence of the slow vertical mixing in the SBL and the "unmixed" mean wind profiles is the relative importance of the lateral mean wind and wind direction shear or wind "turning" with height. For plume transport, this results in a mean lateral displacement relative to the boundary layer averaged wind direction, which is oriented in the x direction for the dispersion calculations. Figure 6 shows crosswind profiles of the vertically-integrated concentration (VIC) C^z at five downstream locations, where $C^z = \int_0^\infty C(x, y, z)dz$. The maximum VIC along a crosswind profile is a rough measure of the mean lateral displacement, which ranges up to $\sim 2z_i$ at the most distant location, $X = 0.9$. Figure 6 also shows the evolving skewness of the crosswind profile with increasing distance, i.e., a longer tail exists on
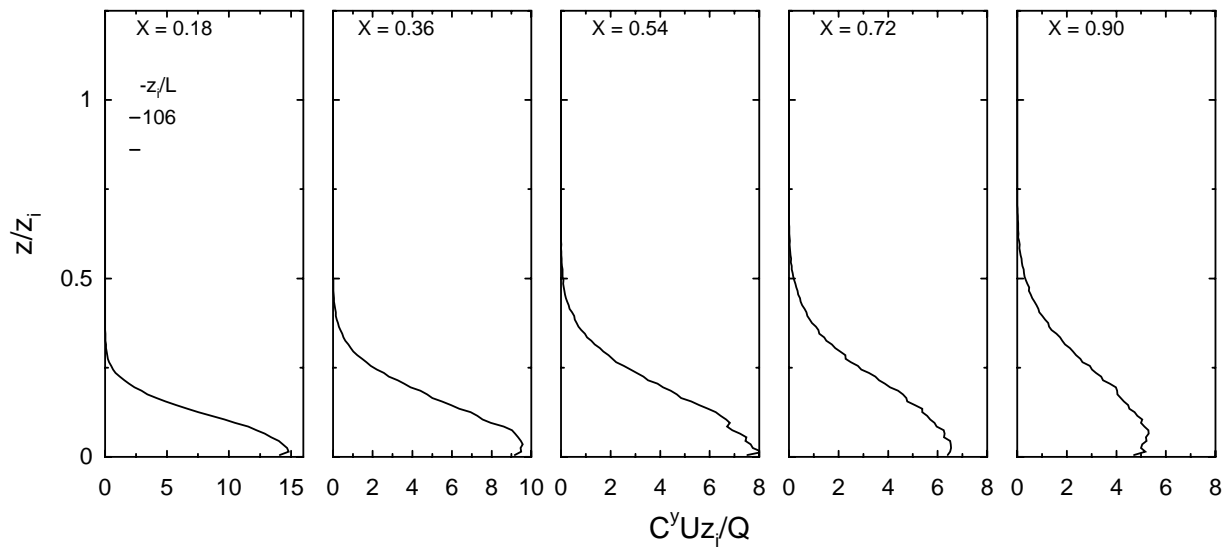
Figure 4: Vertical profiles of the dimensionless CWIC at five downstream distances for a surface release.
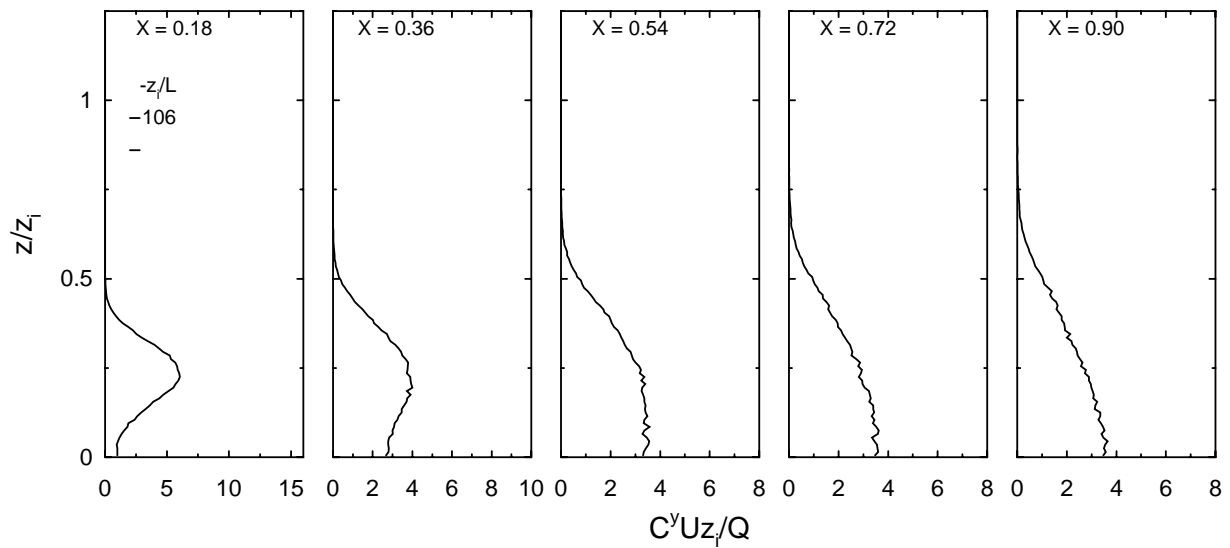
Figure 5: Vertical profiles of the dimensionless CWIC at five downstream distances for an elevated release at $z_s/z_i = 0.24$.
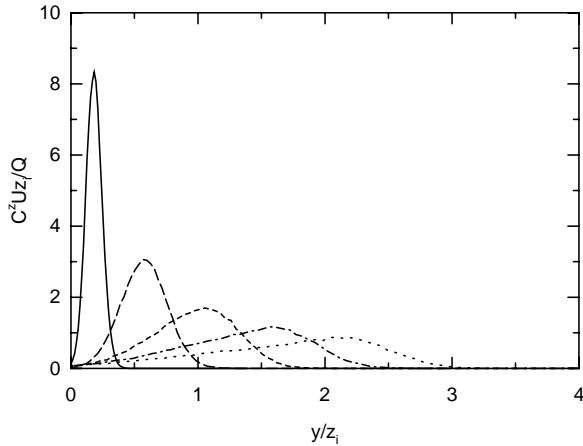
Figure 6: Crosswind profiles of the dimensionless vertically-integrated concentration at five downstream distances for an elevated source at $z_s/z_i = 0.24$; solid, long dashed, short dashed, dot-dashed, and dotted lines correspond to profiles at $X = 0.1$, 0.3, 0.5, 0.7 and 0.9, respectively.

the left side of the maximum than on the right. Furthermore, one can observe a plume that is much wider (in y) than it is tall; e.g., at $X = 0.7$, the plume spans $2.5z_i$ in y whereas its vertical depth is only $\sim 0.5z_i$ (Fig. 5) at the same distance.

Figure 7 presents the dimensionless mean plume height $\overline{z_p}/z_i$ as a function of X for source heights ranging from zero to $z_s/z_i = 0.24$. Overall, the computed growth in $\overline{z_p}$ is rather slow. For the surface source, the mean height can be approximated by $\overline{z_p}/z_i = 0.2X^{1/2}$ far downstream, which suggests that the plume centroid would reach the middle of the SBL at $X = 12.5$ or at a distance of 64 km! This of course assumes that no other mechanisms (e.g., mesoscale processes, dispersion in hill wakes, etc.) would be operating. Nevertheless, the growth is impressively slow. For the elevated sources, there is an initial negative displacement followed by a tendency toward the surface source result at large distances.

The computed growth rate, $\overline{z_p} \propto x^{1/2}$, is faster than that given by surface layer similarity (SLS) theory far downstream, where SLS predicts $\overline{z_p} \propto x^{1/3}$ (van Ulden, 1978). The faster growth in our calculations may be explained by the rather weak stability; for example, at a height of $z/z_i = 0.2$ which exceeds the $\overline{z_p}/z_i$ values found for the surface source in Fig. 7, the corresponding z/L is only ~ 0.3. In contrast, the above SLS result applies to strongly stable conditions where $z/L \gg 1$ or in "z-less stratification."

The analysis in Section 3.1 supported the adoption of ℓ_b and N^{-1} as the turbulence length and time scales.
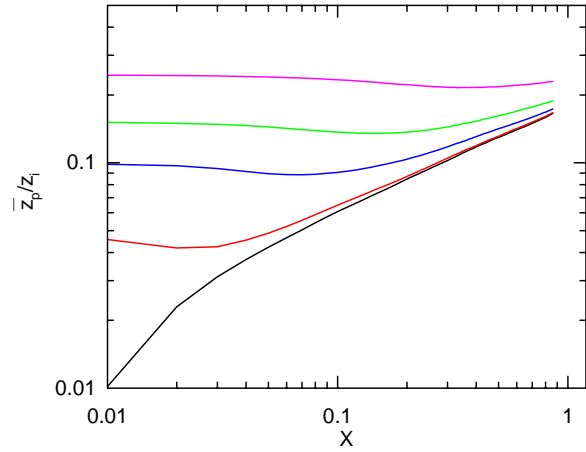
Figure 7: Dimensionless mean plume height as a function of dimensionless distance for five source heights in the SBL; black, red, blue, green, and magenta lines correspond to releases at $z_s/z_i = 0.0026$, 0.047, 0.10, 0.15 and 0.24, respectively.
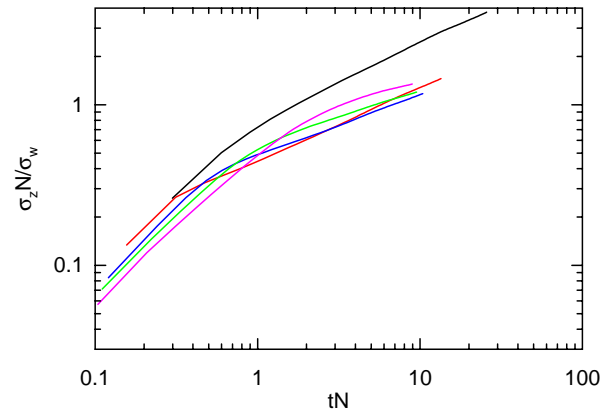
Figure 8: Dimensionless vertical dispersion as a function of dimensionless time for five source heights in the SBL; black, red, blue, green, and magenta lines correspond to releases at $z_s/z_i = 0.0026$, 0.047, 0.10, 0.15 and 0.24, respectively.

In the following, we examine the vertical dispersion σ_z about the mean plume height using the dimensionless coordinates $\sigma_z N/\sigma_w$ and tN^{-1}. This also follows from considering two statistical theories for dispersion. The first is Taylor's theory which Venkatram et al. (1984) adopted and chose a simple interpolation expression that matched the short- and long-time limits of the theory:

$$\sigma_z = \frac{\sigma_w t}{(1 + 0.5t/T_L)^{1/2}}, \qquad (4)$$

where $\sigma_z = \sigma_w t$ for $t \ll T_L$ and $\sigma_z = (2\sigma_w^2 T_L t)^{1/2}$ for $t \gg T_L$. Venkatram et al. assumed $T_L = \ell/\sigma_w$ and chose an interpolation expression for ℓ that followed $\ell \propto z$ near the surface and $\ell \propto \ell_b$ above the surface layer.

The second theory by Pearson et al. (1983) also predicted $\sigma_z = \sigma_w t$ for short times, but for large times $(t \gg N^{-1})$, it gave

$$\sigma_z = \frac{\sigma_w}{N}(c_1^2 + 2N^2 T_L t)^{1/2}. \qquad (5)$$

Here, $c_1 \simeq 1.3$, $T_L \sim \gamma^2 N^{-1}$, and γ is a dimensionless parameter that measured the degree of mixing between fluid elements. For $\gamma \sim 0.1$, σ_z approached a constant $\sim \sigma_w N^{-1}$ over a considerable range of time, but for $\gamma \geq 0.3$, σ_z approached a $t^{1/2}$ dependence. From the data reported by Venkatram et al. (1984), both a constant σ_z and a $\sigma_z \propto t^{1/2}$ behavior have been deduced for elevated plumes.

Figure 8 shows the dimensionless vertical dispersion $\sigma_z N/\sigma_w$ versus tN^{-1} from the Lagrangian particle simulations for source heights ranging from ~ 0 to $0.24 z_i$. The σ_w and N in this scaling are the source height values. The results show that the dispersion from all source heights tends to the short-time limit for $tN^{-1} \ll 1$, but they fall roughly into two groups for $tN^{-1} > 1$. The surface source follows $\sigma_z \propto t^{1/2}$, whereas the other results collapse into a band exhibiting $\sigma_z \propto t^{1/3}$ approximately. This is intermediate to the classical and Pearson et al. very stable limits. Further analysis is necessary to understand and explain this behavior.

REFERENCES

Barad, M. L., 1958: Project prairie grass. A field program in diffusion, Technical Report AFCRF-TR-235, Air Force Cambridge Research Center, Bedford, MA.

Beare, R. J., M. K. Macvean, A. A. M. Holtslag, J. Cuxart, I. Esau, J.-C. Golaz, M. A. Jimenez, M. Khairoutdinov, B. Kosovic, D. Lewellen, T. S. Lund, J. K. Lundquist, A. Mccabe, A. F. Moene, Y. Noh, S. Raasch, and P. P. Sullivan, 2005: An intercomparison of large-eddy simulations of the stable boundary layer, *Boundary-Layer Meteorol.*, **in press**.

Brost, R. A. and J. C. Wyngaard, 1978: A model study of the stably stratified planetary boundary layer, *J. Atmos. Sci.*, **35**, 1427–1440.

Brown, A. R., S. H. Derbyshire, and P. J. Mason, 1994: Large-eddy simulation of stable atmospheric boundary layers with a revised stochastic subgrid model, *Quart. J. Roy. Meteorol. Soc.*, **120**, 1485–1512.

Horst, T. W., 1979: Lagrangian similarity modeling of vertical diffusion from a ground-level source, *J. Appl. Meteorol.*, **18**, 733–740.

Kemp, J. R. and D. J. Thomson, 1996: Dispersion in stable boundary layers using large-eddy simulation, *Atmos. Environ.*, **30**, 2911–2923.

Kosovic, B. and J. A. Curry, 2000: A large eddy simulation of quasi-steady, stably stratified atmospheric boundary layer, *J. Atmos. Sci.*, **57**, 1052–1068.

Lamb, R. G., 1978: A numerical simulation of dispersion from an elevated point source in the convective boundary layer, *Atmos. Environ.*, **12**, 1297–1304.

Moeng, C.-H. and P. P. Sullivan, 1994: A comparison of shear and buoyancy driven planetary-boundary-layer flows, *J. Atmos. Sci.*, **51**, 999–1022.

Nieuwstadt, F. T. M., 1984a: Some aspects of the turbulent stable boundary layer, *Boundary-Layer Meteorol.*, **30**, 31–54.

—, 1984b: The turbulent structure of the turbulent stable boundary layer, *J. Atmos. Sci.*, **41**, 2202–2216.

Pearson, H. J., J. S. Puttock, and J. C. R. Hunt, 1983: A statistical model of fluid-element motions and vertical diffusion in a homogeneous stratified turbulent flow, *J. Fluid Mech.*, **129**, 219–249.

Sullivan, P. P., J. C. McWilliams, and C.-H. Moeng, 1994: A subgrid-scale model for large-eddy simulation of planetary boundary-layer flows, *Boundary-Layer Meteorol.*, **71**, 247–276.

Taylor, G. I., 1921: Diffusion by continuous movements, *Proc. London Math. Soc.*, **20**, 196–211.

van Ulden, A., 1978: Simple estimates for vertical dispersion from sources near the ground, *Atmos. Environ.*, **12**, 2125–2129.

Venkatram, A., D. Strimaitis, and D. Dicristofaro, 1984: A semiempirical model to estimate vertical dispersion of elevated releases in the stable boundary layer, *Atmos. Environ.*, **18**, 923–928.

Weil, J. C., P. P. Sullivan, and C.-H. Moeng, 2004: The use of large-eddy simulations in lagrangian particle dispersion models, *J. Atmos. Sci.*, **61**, 2877–2887.

Wyngaard, J. C., 1988: Structure of the PBL, in *Lectures on Air Pollution Modeling*, edited by A. Venkatram and J. Wyngaard, pp. 9–61, American Meteorological Society.